Barcelona atmospheric monitoring with lidar: first measurements with the UPC's scanning portable lidar

Cecilia Soriano[a], Francesc Rocadenbosch[b], Alejandro Rodríguez[b], Constantino Muñoz[b], David García-Vizcaíno[b], José M. Baldasano[a] and Adolfo Comerón[b]

[a]Universitat Politècnica de Catalunya (UPC). Laboratory of Environmental Modeling. Dep. of Engineering Projects. Av. Diagonal 647,10.23. 08028. Barcelona, Spain
[b]Universitat Politècnica de Catalunya (UPC). Dep. of Signal Theory and Communications. Group of Antennas, Microwaves, Radar and Optics. C/Gran Capità s/n, D4. 08034 Barcelona, Spain

EUROPTO. Remote Sensing of Clouds and the Atmosphere V. SPIE Proceedings vol. 4168 (2001)

ABSTRACT

Results presented in this contribution correspond to the first measurements made with the transportable lidar system developed by the Universitat Politècnica de Catalunya, which were collected during the year 2000 in the city of Barcelona. The system uses a Nd:YAG laser at 1064 nm wavelength and 0.35 J pulse energy at a 20 Hz pulse repetition rate, has a 20 cm diameter telescope and a scanning range of 120° in elevation and 300° in azimuth. In this study only vertical profiles of atmospheric extinction will be shown. Data were acquired under several meteorological situations, showing the influence that this factor has in the arrangement of aerosols in the vertical dimension, and the distributions of backscatter extinction coefficients obtained from the lidar. Data have also been compared to radiosonde profiles acquired in Barcelona at a near time and have shown how the vertical arrangement of aerosols is correlated with changes in atmospheric stability condition, water content and wind direction.

Keywords: Elastic Backscatter, mobile lidar, urban atmosphere, aerosols, synoptic meteorological situation.

1. INTRODUCTION

Regions with complex orography and a strong coastal influence develop a very wide range of meteorological phenomena that makes them very interesting to study. The main processes going on in coastal environments are daytime convective vertical mixing, sea-breeze circulations, and circulations produced by mountain and river valley thermal and mechanical effects.

These mesoscale phenomena develop better when the synoptic conditions are weak. However, even under stronger synoptic forcings, local topography can modify the flow that the synoptic conditions would impose.

In this contribution we study the influence of the synoptic meteorological situation in the vertical arrangement of aerosols observed by elastic-backscatter data. According to the description of the aerosol arrangement observed with the lidar, and with evidence from previous lidar campaigns conducted in Barcelona[1,2], it seems that the different layers of aerosols monitored have experienced different processes during their circulation through the atmosphere and would correspond to different air masses. This suggests that their physical properties (such as temperature or water content) may have changed along their trajectories.

Several reports have detailed how the vertical aerosol distribution is strongly correlated with the atmosphere temperature profile [3,4,5,6] . The top of the mixing layer (ML) is usually capped by a temperature inversion; it forces pollutants emitted at the surface to remain within the ML. In general, aerosol layers are strongly correlated with layers of different stability condition.

In addition, specific humidity is uniform if the atmosphere is well mixed, and water content will differ in the transition from the ML to a different mass of air. If an air mass is well mixed, its corresponding specific humidity profile should be constant

with height. Furthermore, because specific humidity is a highly conservative quantity, it can be used to identify air masses of different origins. In general, the water vapor is concentrated in the lower atmosphere and is mainly due to evaporation from the soil or sea.

Relative humidity profiles are useful in assessing the influence on the backscatter signal of increased aerosol size caused by water absorption. Comparison of the lidar profiles and relative humidity profiles showed that, in general, an increase in relative humidity corresponds to an increase in range-corrected backscatter. How aerosols swell with increasing relative humidity has been well documented[7,8]. At low relative humidity particles can aggregate molecules of water by adsorption only. At high relative humidity, however, particles grow by absorption of water molecules, increasing their radii, and therefore their backscatter cross-section. According to the high values of relative humidity registered in Barcelona (i.e. because of its seaside location) one can assume that humidity effects can be important on the lidar data through a swelling of the aerosols and an increase of its effective cross-section. This swelling would cause an increase in the backscattered lidar signal that would not correspond to an increase in the concentration of aerosols.

Finally, we also compare extinction profiles with radiosonde profiles of wind direction and speed. This comparison is useful to confirm the different origin of the layer identified with the lidar profiles and with the temperature and humidity profiles, showing the different directions from were the different air layers have come.

In this contribution, radiosonde data has been compared with vertical profiles of extinction coefficients extracted from elastic-backscatter lidar data and under different dominating synoptic conditions, and it is shown how aerosol vertical arrangement is highly dependent on the prevailing atmospheric conditions.

2. THE UPC LIDAR SYSTEM AND THE INVERSION TECHNIQUE

A few years ago the UPC started to develop its own lidar system. The first stage of the project was the construction of an elastic-backscatter lidar. The system was ready to participate in an experimental campaign in the fall of 1996. The results we show in this contribution correspond to the first measurements acquired with the mobile system, and were collected during the year 2000 in the city of Barcelona. Some of the specifications of the system are: Nd:YAG laser at 1064 nm wavelength and 0.35 J pulse energy at a 20 Hz pulse repetition rate, telescope diameter of 20 cm, and scanning range of 120° in elevation and 300° in azimuth. Figure 1 shows a picture of the UPC lidar system. However, for this contribution we will only use vertical profiles of lidar data acquired at constant elevation angle. In fact, part of the measurements were conducted in the framework of the EARLINET project, an EU-funded initiative whose aim is the creation of a network of lidar systems acquiring data simultaneously all over Europe on a regular basis[9], and are also part of the IMMPACTE project, funded by the Catalan Department of the Environment.

Fig.1 The UPC lidar system

EUROPTO. Remote Sensing of Clouds and the Atmosphere V. SPIE Proceedings vol. 4168 (2001)

Inversion of the lidar signal is based on the Klett-Fernald-Sasano algorithm from which the atmospheric extinction and backscatter profiles are obtained.

The Klett-Fernald-Sasano algorithm is a modification of the Klett inversion algorithm which includes Rayleigh terms and a non-constant extinction-to-backscatter ratio. Under such conditions, the following expression is obtained from the lidar equation:

$$\beta_M(z) = \frac{P(z)z^2 \exp\left\{+2\int_z^{z0}[S_M(u) - S_R(u)]\beta_R(u)du\right\}}{\frac{P(z_0)z_0^2}{\beta_M(z_0)+\beta_R(z_0)} + 2\int_z^{z0} S_M(u)P(u)u^2 du \exp\left\{2\int_u^{z0}[S_M(v) - S_R(v)]\beta_R(v)dv\right\}} - \beta_R(z)$$

where:

$$S_R = \frac{8\pi}{3}; \quad \beta(z) = \beta_R(z) + \beta_M(z) = \frac{\alpha_R(z)}{S_R} + \frac{\alpha_M(z)}{S_M(z)}$$

$$\alpha_R(z,\lambda,P,T) \approx \alpha_R^{sca}(z,\lambda,P,T) = \frac{8\pi^3\left(m_{air}^2(z,P.T)-1\right)^2}{3\lambda^4 N_S^2(0)} \cdot \frac{6+3\gamma}{6-7\gamma} \cdot N_S^2(z,P,T)$$

Terms with *R* subscript indicate Rayleigh scattering contributions, while subscript *M* is associated with particles (Mie scattering).

3. CASE #1: COLD AIR POOL ALOFT, MAY 8, 2000.

The synoptic charts of Figure 2 show the sea-level pressure and 500 hPa geopotential height at 12 GMT on May 8, 2000. The cold air pool synoptic situation can be identified in the synoptic charts because they show a low pressure area in the 500 hPa chart, which is not obvious in the surface chart, indicating a concentration of cold air.

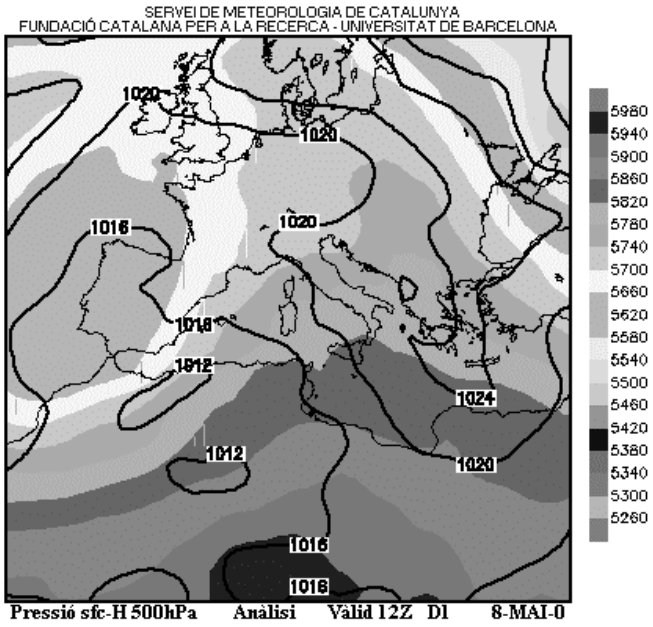

Fig. 2. Synoptic charts for May 8, 2000 at 12 GMT. Isolines indicate sea-level pressure and shaded areas indicate geopotential heights at 500 hPa.

EUROPTO. Remote Sensing of Clouds and the Atmosphere V. SPIE Proceedings vol. 4168 (2001)

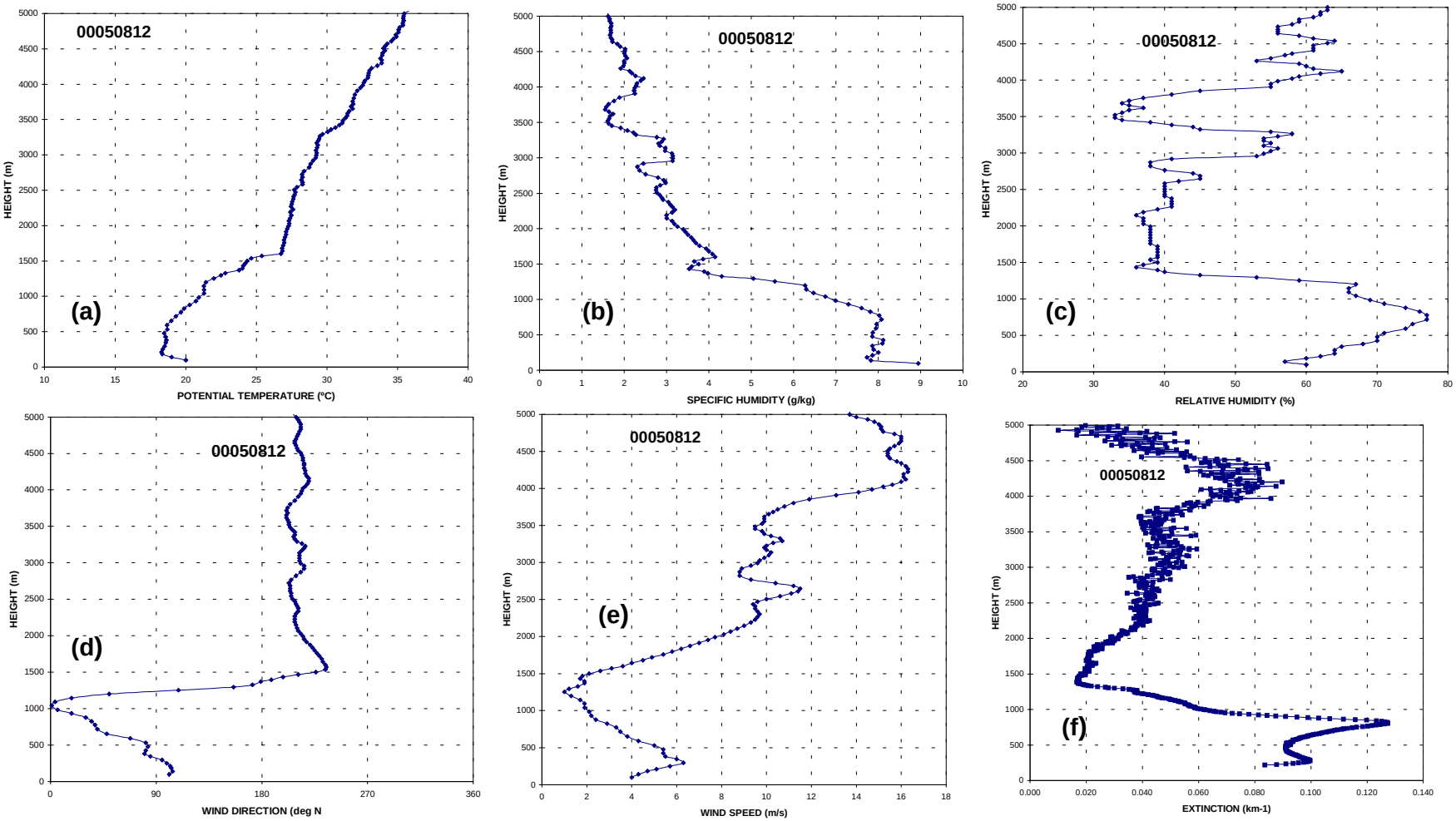

Fig. 3 Vertical profiles of potential temperature (a), specific humidity (b), relative humidity (c), wind direction (d), wind speed (e), measured by a radiosonde launched in Barcelona at 12 GMT on May 8, 2000, and the vertical profile of atmospheric extinction extracted from elastic lidar measurements (f).

Fig. 3 shows the corresponding profiles acquired by the radiosonde launched at 12 GMT and the vertical profile of atmospheric extinction inferred from elastic-backscatter data acquired at the same time. Lidar data show a layered structure that can be divided into four main different layers: a first layer of high lidar return and therefore high extinction coefficient situated from the surface level up to about 500 m. A second layer is situated around 1000 m height. Increased extinction is observed again between 2000 and 3500 m, and a fourth layer is located between 4000 and 4500 m.

This layered structure can also be seen in the profiles of different atmospheric variables recorded by radiosonde, indicating that they are indeed different atmospheric layers that have undergone different atmospheric processes. For instance, the layer starting near the surface is located in a neutrally-stratified region (well mixed) that is capped by a sudden stabilization of the atmosphere that can be observed in the potential temperature profile from the radiosonde. However, the layer observed just below 1000 m is located in a more stable region. An important temperature inversion is observed between 1200 and 2000 m. This layer wouldn't allow aerosols from the surface to reach higher levels.

An increase in the extinction coefficient is found above that height, indicating a high load of aerosols. It is important to note the lower water content of this layer with respect to the one in the inferior layers. While specific humidity below 1000 m is of the order of 8 g/kg, this elevated layer around 2500 m has a much lower content of roughly 3.5 g/kg. This sudden change in specific humidity indicates that the two layers correspond to different air masses, and have undergone different atmospheric processes that have changed their water content. In fact, the different origin of these two air masses is confirmed by the vertical profile of wind direction recorded by the radiosonde. The profile shows a sudden change in wind direction between 1000 and 1500 m height. Winds below that height have a general Northeastern component, while above 1500 m winds have changed towards a Southwesterly component. Being located in the Northeastern part of Spain, easterly winds in Barcelona have a sea origin which explains the higher water content in the lower atmosphere.

4. CASE #2: TROUGH , JUNE 5, 2000.

The synoptic charts included in Figure 4 show the sea-level pressure and 500 hPa geopotential height at 12 GMT on June 5, 2000. Charts show a clearly formed trough at 500 hPa to the north of the Iberian Peninsula, indicating the pass of a cold front.

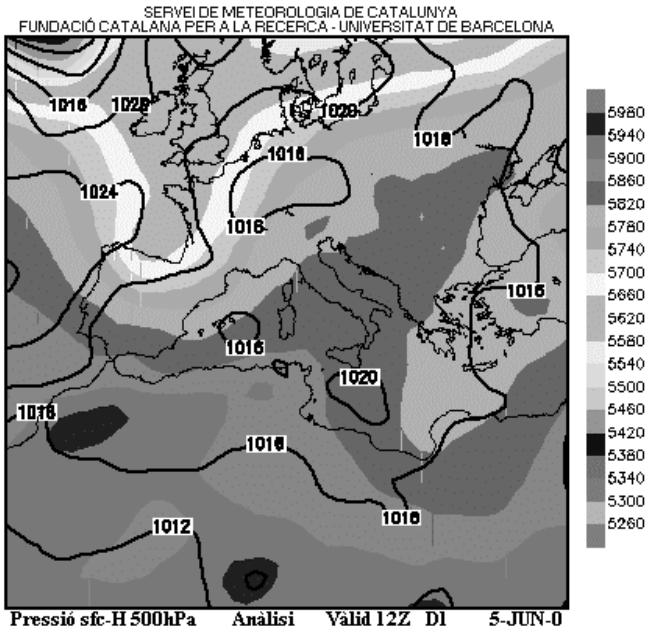

Fig. 4. Synoptic charts for June 5, 2000 at 12 GMT. Isolines indicate sea-level pressure and shaded areas indicate geopotential heights at 500 hPa

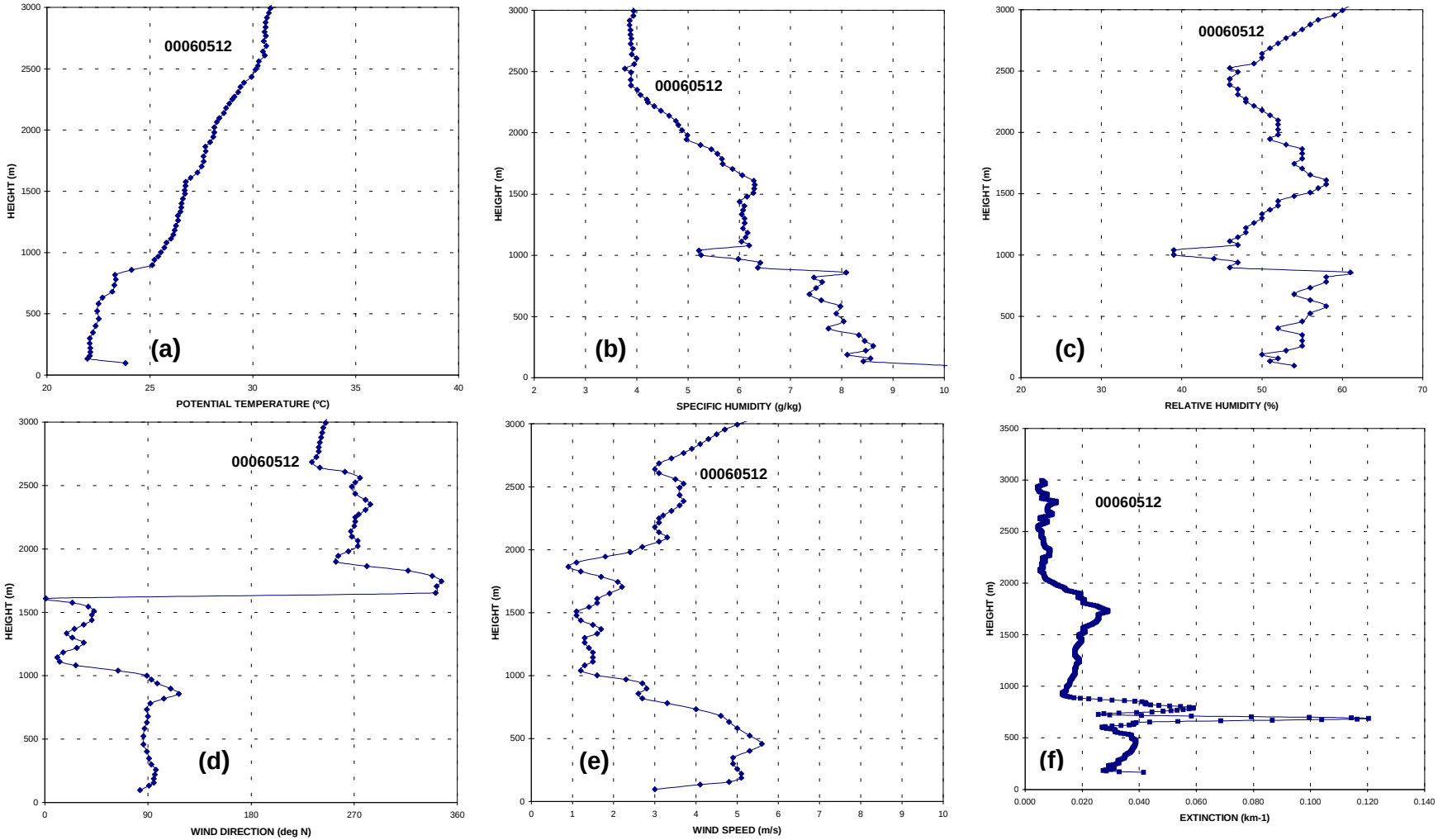

Fig. 5 Vertical profiles of potential temperature (a), specific humidity (b), relative humidity (c), wind direction (d), wind speed (e), Measured by a radiosonde launched in Barcelona at 12 GMT on June 5, 2000, and the vertical profile of atmospheric extinction at 12 GMT extracted from elastic lidar measurements (f).

Fig. 5 shows the vertical profile of atmospheric extinction inferred from elastic-backscatter data acquired at 12 GMT on June, 5, 2000 (bottom right). The profile is compared with the radiosonde launched at that time.

The extinction profile shows a two-layer structure of aerosols; a first layer up to about 800 m, and a second layer with increased extinction between 1100 and 2000 m. The important and very local increase of atmospheric extinction around 600 m probably corresponds to the presence of a very narrow layer of clouds.

The temperature inversion shown by the potential temperature around 800 m clearly indicates the limit of the first layer of aerosols. These surface-related aerosols have a higher water content than the layer situated immediately above (the reduction is of the order of 2 g/kg). The rather constant temperature profile and specific humidity in that layer are an indicator of the important mixing going on. Again, the change of atmospheric layer is also indicated by the sudden change in the wind direction. Winds below 900 m have an easterly component, indicating a marine origin which would explain its higher water content.

Above 1100 m height aerosol load begins to increase again, although atmospheric extinction is lower in this layer (around 0.02 km^{-1}). Note that this layer is also situated in a region with rather neutral stabilization, and is limited above and below by important temperature inversions that do not allow the dispersion and mixing in the vertical dimension. Winds in that layer have a general northerly component, and the mixing is important and is also indicated by the almost constant specific humidity value of 6 g/kg.

Finally, wind changes direction again above 2000 m, where it adopts a westerly component, water content is dropping to 4 g/kg and atmospheric extinction is very low. The value of atmospheric extinction is very low, showing a small bump above 2500 m that would correspond to the neutral stabilization layer found at that height.

5. CASE #3: NORTHEASTERN ADVECTION , JUNE 15, 2000.

The synoptic charts included in Figure 6 show the sea-level pressure and 500 hPa geopotential height at 12 GMT on June 15, 2000. Charts show that a high pressure area located to the NW of France provokes NE winds above Catalonia. Isohipses in height also induce a NE flow.

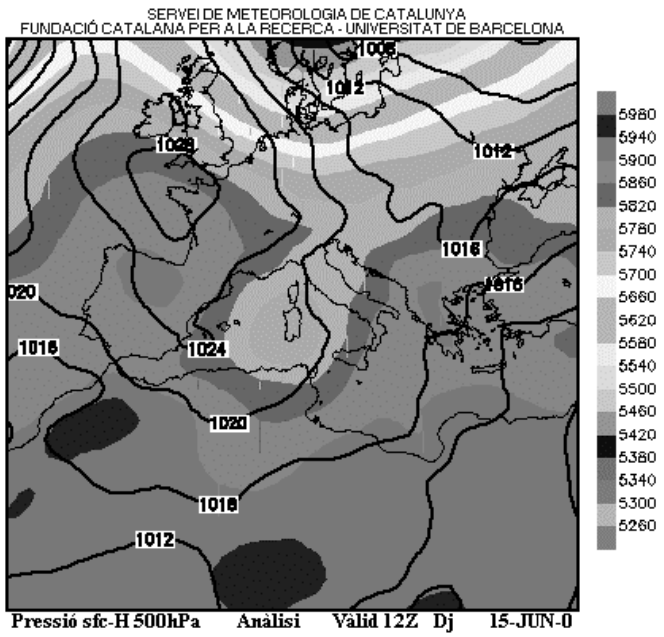

Fig. 6. Synoptic charts for June 15, 2000 at 12 GMT. Isolines indicate sea-level pressure and shaded areas indicate geopotential heights at 500 hPa.

EUROPTO. Remote Sensing of Clouds and the Atmosphere V. SPIE Proceedings vol. 4168 (2001)

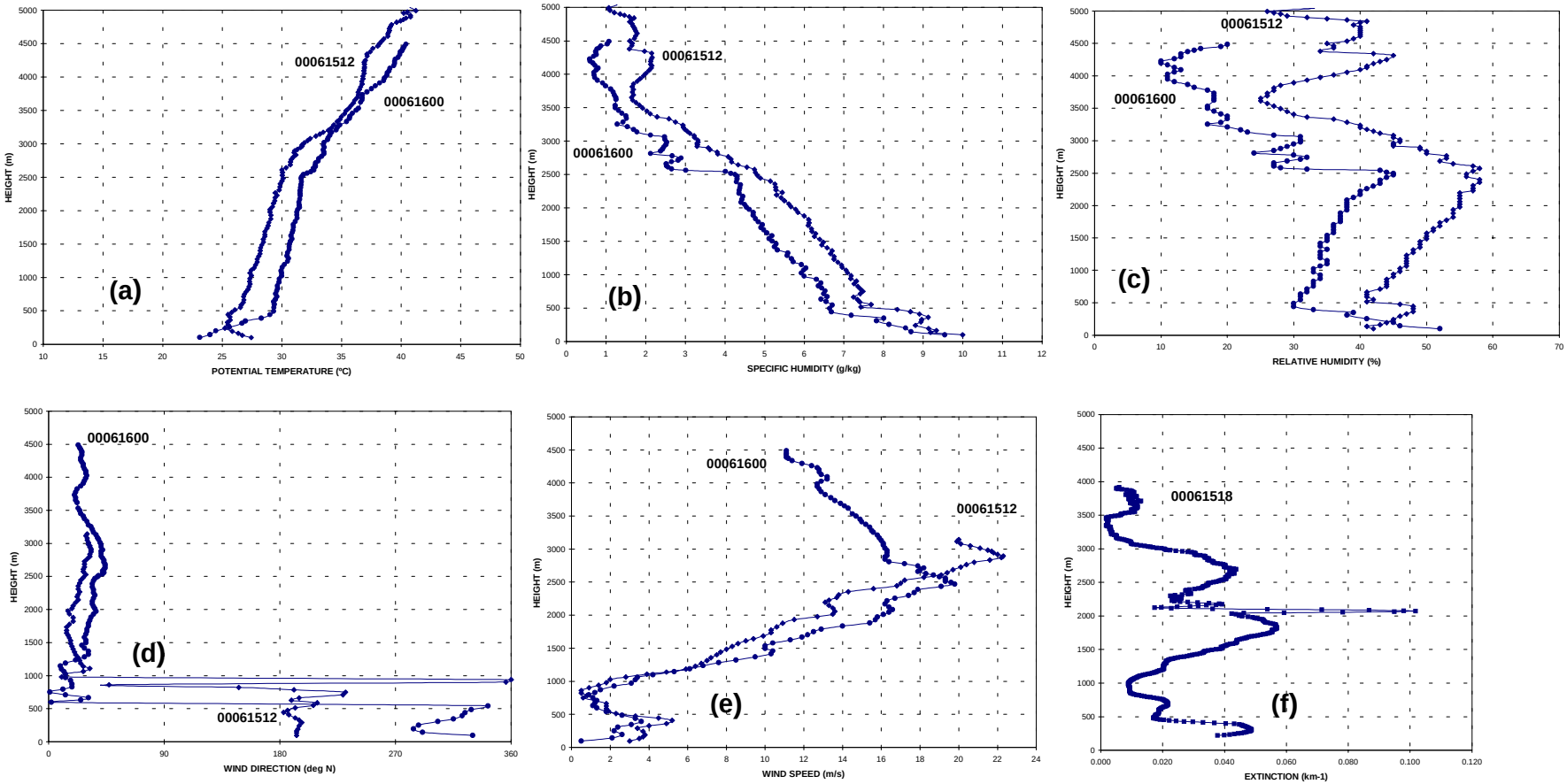

Fig. 7 Vertical profiles of potential temperature (a), specific humidity (b), relative humidity (c), wind direction (d), wind speed (e), measured by the radiosonde launched in Barcelona at 12 GMT on June 15, 2000 (diamonds), and at 00 GMT on June 16, 2000 (circles). Vertical profile of atmospheric extinction at 18 GMT extracted from elastic lidar measurements (f).

Fig. 7 shows the vertical profile of atmospheric extinction inferred from elastic-backscatter data acquired at 18 GMT on June, 15, 2000 (bottom right). Since no radiosonde was launched at that time, the profile is compared with radiosonde data acquired at 12 GMT the same day and the following midnight (00 GMT June, 16, 2000). The profile acquired by the lidar would thus correspond to a situation in-between the two shown.

However, radiosonde profiles at those two times do not differ very much. The main difference is observed in the potential temperature profile, which shows a general subsidence of the air masses due to the prevailing anticyclonic conditions. Note, for instance, how the temperature inversion identifiable at 3000 m in the 12 GMT profile is situated at 2500 m at midnight. Next to the surface, it is also remarkable the change from a superadiabatic condition at noon to a highly stable situation at noon. In both cases, however, a temperature inversion at about 500 m marks the depth of the layer where surface emitted aerosols are kept.

Above this height we find a sudden change in the wind direction, which shifts to take a Northeasterly direction. Note also the increase in wind speed. Atmospheric extinction picks up again, from 1000 up to 3000 m. In the temperature profile this region looks like and almost neutral layer, and water content is gradually decreasing with height. We are not sure if the high peak observe in the lidar profile at 2000 m corresponds to and accumulation of aerosols. The fact that neither the temperature profiles nor the wind direction or humidity profiles show any special feature at that time makes us think that this peak may have been caused by a thin cloud that condensed during the 30 minute period that the lidar was acquiring data.

Finally, note that the small bump observed at 3500 m in the extinction profile at 18 GMT seems to correspond with the neutral layer observed between 3700 and 4000 m in the temperature profile at 12 GMT

6. CASE #4: SOUTHERN ADVECTION , JUNE 19, 2000.

The synoptic charts included in Figure 8 show the sea-level pressure and 500 hPa geopotential height at 12 GMT on June 19, 2000. Charts show how isobars are orientated from north to south, indicating a general southern flow usually associated with higher temperatures and bad visibility.

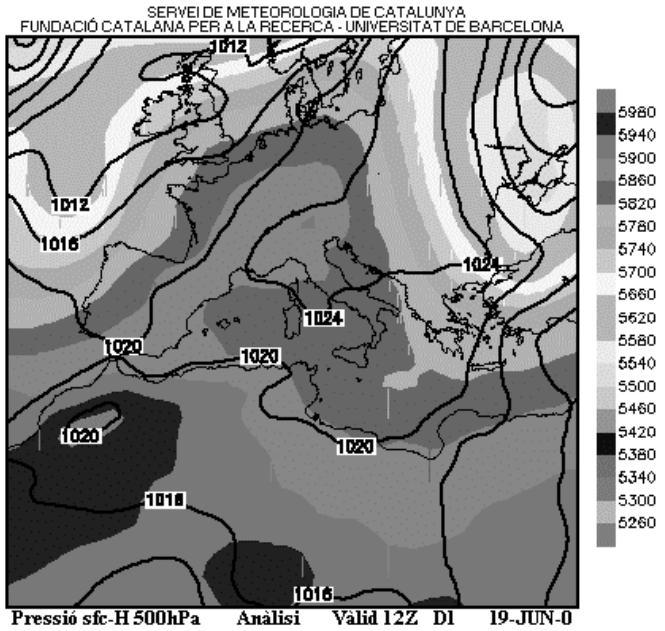

Fig. 8. Synoptic charts for June 19, 2000 at 12 GMT. Isolines indicate sea-level pressure and shaded areas indicate geopotential heights at 500 hPa

EUROPTO. Remote Sensing of Clouds and the Atmosphere V. SPIE Proceedings vol. 4168 (2001)

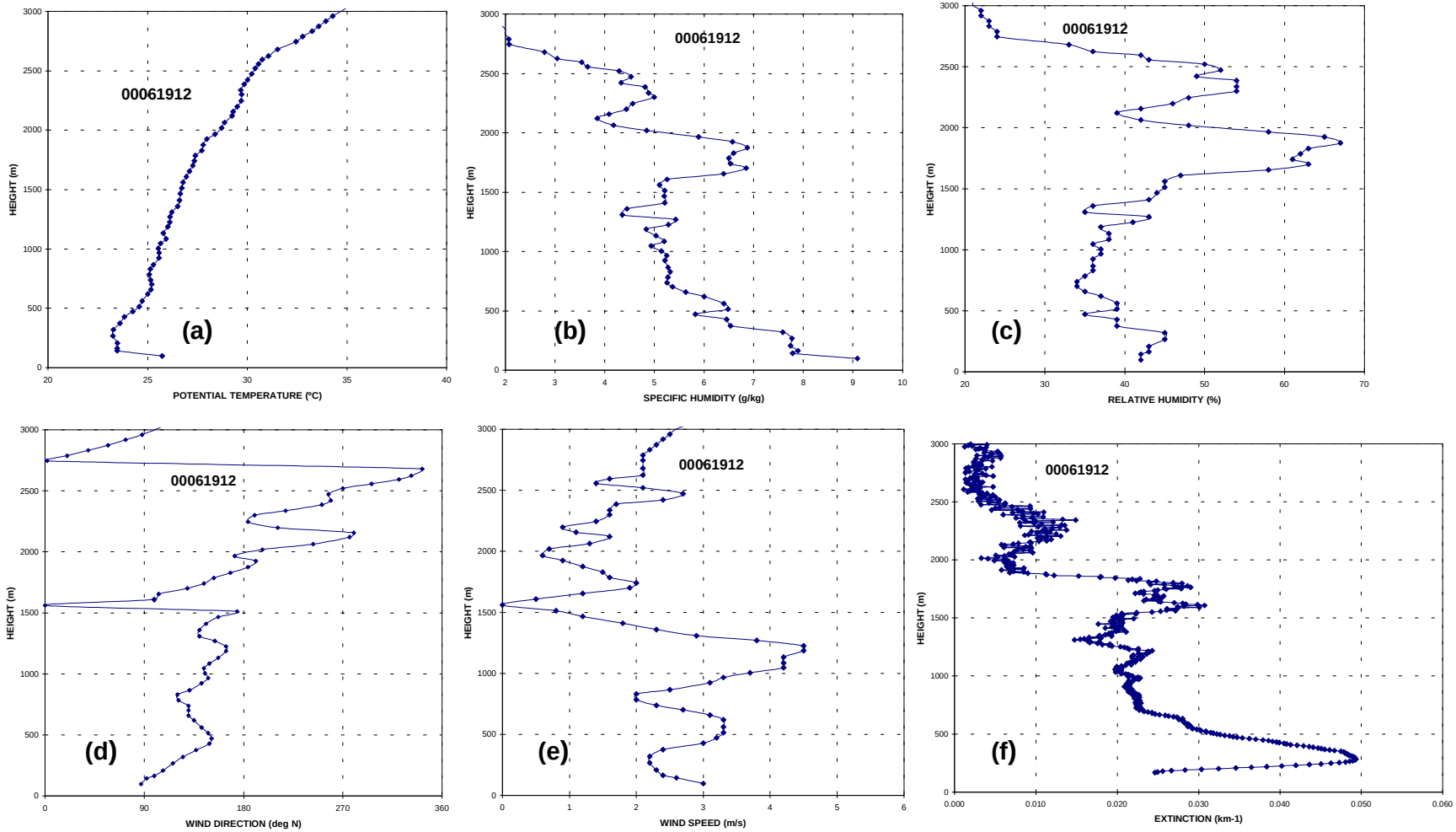

Fig. 9 Vertical profiles of potential temperature (a), specific humidity (b), relative humidity (c), wind direction (d), wind speed (e), measured by a radiosonde launched in Barcelona at 12 GMT on June 19, 2000, and vertical profile of atmospheric extinction at 12 GMT extracted from elastic lidar measurements (f).

Fig. 9 shows the vertical profile of atmospheric extinction inferred from elastic-backscatter data acquired at 12 GMT on June, 19, 2000 (bottom right). The profile is compared with the data of the radiosonde launched at that time.

The extinction profile for that date shows a rather complex layered structure where regions of high aerosol content alternate with layers of very low atmospheric extinction. In general, this layered structure is correlated with regions of stable and unstable atmosphere revealed by the temperature profile. The latter shows a temperature inversion at 500 m, which coincides with the reduction of aerosol content shown by the lidar in the layer starting at the surface. That height would indicate the depth of the mixing layer (note the almost vertical temperature profile).

Specific humidity drops from 8 to 5 g/kg above that altitude. Extinction begins to increase above 700 m up to 2000 m. The layer observed coincides with an almost neutral region that is limited below by the temperature inversion at 500 m and the sudden stabilization at 2000 m. Winds are mostly of the South-Southeasterly component. Increased backscatter within that layer between 1500 and 2000 m is difficult to explain in terms of a stabilization change, since this is not evident to deduce from the potential temperature profile, but it is highly correlated to the increased relative humidity, which probably would mean that not all the increased lidar signal is due to increased aerosol content. However, this kind of assertions are difficult to make with signals from an elastic-backscatter lidar, and additional information about the particle size distribution is necessary to identify with security where aerosol content has increased.

7. CONCLUSIONS

This contribution has shown how different atmospheric synoptic situations lead to different arrangement of atmospheric aerosols and how this arrangement is strongly related to the structure of the atmosphere in terms of stability, water content and wind direction.

Profiles of atmospheric extinction can be very different from one day to the other, both in number of layers observed and in the actual value of the extinction coefficient itself. One important thing that this long term study has shown so far is that vertical arrangement of aerosols is rather distant from the classical structure of a mixing layer next to the surface and clean air above it. Several transport mechanisms ranging from the global/synoptic range to the mesoscale/local range participate in the process and play an important role in the final arrangement of the aerosols in the vertical dimension.

Further investigation will have to be carried out in order to confirm if similar arrangements take place under similar synoptic conditions. In fact, the multilayer arrangement of aerosols and its interpretation have already been confirmed for a typical summertime situation in Barcelona[2]. Also, simulation with numerical models of the different typical synoptic situations analyzed will be useful to assess the different atmospheric mechanisms leading to the arrangements found from which circulatory patterns can be inferred[1].

8. ACKNOWLEDGMENTS

Part of this work has been conducted in the frame of the EU-funded project EARLINET and of the IMMPACTE project, an initiative funded by the Department of the Environment of the Generalitat de Catalunya.

9. REFERENCES

1. Soriano, C., Baldasano, J.M., Buttler, W.T. and Moore, K. Circulatory patterns of air pollutants within Barcelona Air Basin in a summertime situation: lidar and numerical approaches. *Boundary-Layer Meteorol*. In press, 2000.
2. Soriano, C., Rocadenbosch, F., Puente, C., Rodríguez, A., Baldasano, J.M. and Comerón, A. Confirmation of a Multilayer Arrangement of Aerosols in the Barcelona Air Basin Using Two Independent Lidar Systems. In: Spectroscopic Atmospheric Environmental Monitoring Techniques, (Ed: Schäfer, K). SPIE Proceedings Series, Volume 3593, pp. 212-222, 1998.
3. Endlich, R. H., F. L. Ludwig, and E. E. Uthe, An automatic method for determining the mixing layer depth from lidar observations, *Atmos. Environ*.,13, 1051-1056, 1979.

4. Coulter, R. L., A comparison of three methods for measuring mixing-layer height. *J. Appl. Meteorol.*, 18, 1495-1499, 1979.
5. Sasano, Y., A. Shigematsu.,H. Shimizu, N. Takeuchi and M. Okuda, On the relationship between the aerosol layer height and the mixed layer height determined by laser radar and low-level radiosonde observations, *J. Meteorol. Soc. Jap.*, 60, 889-895, 1982.
6. Van Pul, W. A. J., A. A. M. Holstag and D. P. J. Swart, A comparison of ABL heights inferred routinely from lidar and radiosondes at noontime, *Boundary-Layer Meteorol.*, 68, 173-191, 1994.
7. Werner, C., Lidar measurements of atmospheric aerosol as a function of relative humidity, *Opto-elect.*, 4, 125-132, 1972.
8. Dupont, E., J. Pelon, and C. Flamant, Study of the convective boundary-layer structure by scattering lidar, *Boundary-Layer Meteorol.*, 69, 1-25, 1994.
9. Bösenberg *et al*., EARLINET: A European Aerosol Research Lidar Network. 20th International Laser Radar Conference. 10-14 July, 2000. Vichy, France.

EUROPTO. Remote Sensing of Clouds and the Atmosphere V. SPIE Proceedings vol. 4168 (2001)